Talanta 89 (2012) 505–512

Contents lists available at SciVerse ScienceDirect

Talanta

journal homepage: www.elsevier.com/locate/talanta

Molecularly imprinted polymer for the specific solid-phase extraction of kirenol from *Siegesbeckia pubescens* herbal extract

Fang-Fang Chen[a,b,c], Rui Wang[a,b], Yan-Ping Shi[a,b,*]

[a] Key Laboratory of Chemistry of Northwestern Plant Resources, Lanzhou Institute of Chemical Physics, Chinese Academy of Sciences, Lanzhou 730000, PR China
[b] Key Laboratory for Natural Medicine of Gansu Province, Lanzhou Institute of Chemical Physics, Chinese Academy of Sciences, Lanzhou 730000, PR China
[c] Graduate University of Chinese Academy of Sciences, Beijing 100039, PR China

ARTICLE INFO

Article history:
Received 15 November 2011
Received in revised form
28 December 2011
Accepted 30 December 2011
Available online 4 January 2012

Keywords:
Molecularly imprinted polymers
Solid phase extraction
Kirenol
Diterpenoids
Traditional chinese medicines

ABSTRACT

Molecular imprinted polymers (MIPs) were prepared by thermal polymerization using a non-covalent molecularly imprinting strategy with kirenol as the template, acrylamide (AM) as the functional monomer and ethylene glycol dimethacrylamide (EGDMA) as the cross-linker in the porogen of tetrahydrofuran (THF). The synthesized MIPs were characterized by scanning electron microscopy (SEM) and Fourier transform infrared (FT-IR). Its molecular recognition property was investigated by UV spectrogram. High-pressure liquid chromatography (HPLC) was used for analysis of target analytes. The polymers were evaluated further by batch rebinding experiments, and from the derived isotherms their binding capacity and binding strength were determined. Then the selectivity of the MIPs was checked toward the selected structurally related compounds and the recognition coefficients for kirenol, darutigenol, and ent-2-oxo-15, 16, 19-trihydroxypimar-8(14)-ene (TD) were 2.47, 3.43 and 3.40, respectively. The properties of MIPs for SPE were also evaluated. The results obtained demonstrate that the good imprinting effect and the excellent selectivity of MIPs were obtained. The optimized molecular imprinted SPE procedure was applied to extract kirenol directly from the extracts of the aerial part of *Siegesbeckia pubescens* herb. A selective extraction of kirenol from traditional Chinese medicine (TCM) was achieved with extraction yield of 80.9%.

1. Introduction

Molecularly imprinted polymers (MIPs) are man-made materials with a predetermined selectivity toward a target molecule or a group of structurally related species [1–3]. These highly cross-linked polymers were commonly prepared through the polymerization of the complexes of functional monomers and a template to be imprinted with the matrix-forming monomers [4]. A wide range of molecules can serve as templates, such as nucleosides, analgesics, pesticides, carbohydrates, and steroids. Moreover, MIPs are stable to a wide range of pressure, organic solvents, and pHs [5]. These attributes make MIPs ideal for extensive application in artificial antibodies [6], catalysis [7], drug delivery [8], solid-phase extraction [9], chromatography [10], sensors [11], and sorbent assays [12]. In the recent decades, MIPs have attracted great research interests because of its huge potential in the application of solid-phase extraction [13–16].

Molecularly imprinted solid-phase extraction (MISPE) procedure was first reported by Sellergren [17]. The main benefit of this procedure is that the selectivity of a MIP for a target compound or a group of compounds can be pre-determined by the choice of template employed for its preparation where the traditional sorbent lack selectivity. High selectivity of the sorbent may lead to efficient sample extraction or clean-up. MISPE can not only concentrate the target molecule, but also remove other compounds present in the sample matrix. Therefore, MISPE has been successfully applied to the extraction and determination of target analytes in different matrices. Most of the MISPE applications have focused on extracting compounds from biological [18–20] and environmental samples [21–24], while a small number of studies have dealt with drug [25], food [26], and other samples. MISPE has also been used to extract active components from complex plant extracts like traditional Chinese medicines (TCMs) [10,27–30].

The aerial parts of the herb *Siegesbeckia pubescens* are extensively used in TCMs for their antiinflammatory, antiallergic, cartilage protective, and wound healing properties [31–36]. Its major active compound is kirenol. Kirenol has been illustrated to antagonize rheumatism by inhibiting inflammation and regulating immune function and apoptotic protein expression in synoviocytes, which is one of the leading natural compounds for clinical trials in

* Corresponding author at: Lanzhou Institute of Chemical Physics, Chinese Academy of Sciences, Lanzhou 730000, PR China. Tel.: +86 931 4968208; fax: +86 931 4968094.
E-mail address: shiyp@licp.cas.cn (Y.-P. Shi).

0039-9140/$ – see front matter © 2012 Elsevier B.V. All rights reserved.
doi:10.1016/j.talanta.2011.12.080

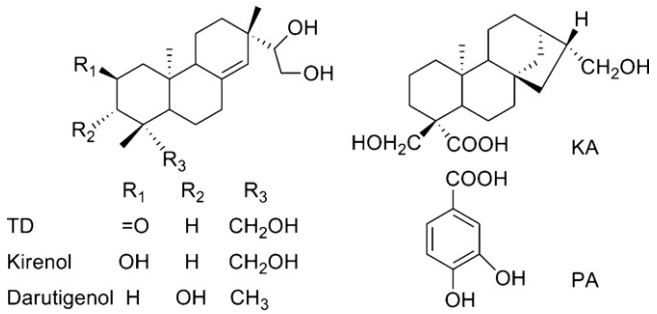

Fig. 1. Structures of PA, kirenol and its analogues.

recent studies on rheumatism [37–39]. The extraction of kirenol from plants, however, is tedious and inefficient because of its poor affinity and selectivity to conventional separation materials. Therefore, developing efficient adsorbent materials with high affinity for kirenol is essential.

In the present work, a MIP was prepared for kirenol (target molecule) using a non-covalent imprinting method employing acrylamide (AM) as functional monomers, and ethylene glycol dimethacrylate (EGDMA) as a cross-linker in tetrahydrofuran porogen. The synthesized MIPs and non-imprinted polymers (NIPs) were characterized via scanning electron microscopy (SEM) and Fourier transform infrared spectrometry (FT-IR). Its molecular recognition property was investigated using UV spectrophotometry. High-pressure liquid chromatography (HPLC) was used to evaluate the adsorption and selectivity properties of the MIPs. The properties of MIPs for SPE were also evaluated. The optimized MISPE procedure was applied to extract kirenol directly from the extracts of the aerial part of *S. pubescens* herb.

2. Experimental

2.1. Materials and regents

Acrylamide (AM), ethylene glycol dimethacrylamide (EGDMA), and 2,2′-azobisissobutyronitrile (AIBN) were obtained from Alfa Aesar (Tianjin, China). Kirenol, darutigenol, ent-2-oxo-15,16,19-trihydroxypimar-8(14)-ene (TD) and ent-17,18-dihydroxy-16βH-kauran-19-oic acid (KA) were provided by our lab [40]. Protocatechuic acid (PA) was provided by the National Institute for Control of Pharmaceutical and Biological Products (Beijing, China). Their structures are shown in Fig. 1. Chromatographic-grade methanol and acetonitrile was purchased from Merck Co. (Darmstadt, Germany), tetrahydrofuran (THF), acetic acid and the other chemicals were supplied from Tianjin Chemical Reagent Co. (Tianjin, China). Deionized water (18 MΩ) was prepared with a water purification system (Shanghai, China). All solutions used for HPLC were filtered through a 0.45 μm filter before use.

The *S. pubescens* herb (Gansu, China) were extracted following Chinese Pharmacopoeia before SPE extraction.

2.2. HPLC analysis

All chromatographic measurements were performed on an HPLC system (HP1200, Agilent, USA) with a diode array detector (DAD). The analytical column was a 250mm × 4.6 mm, 5 μm C_{18} column (Agilent, USA). The mobile phase was consisted of acetonitrile:methanol (90:10, v/v) and water with the linear gradient elution 0–25 min for 30–70% acetonitrile:methanol (90:10, v/v) at a flow rate of 1.0 mL min^{-1}. DAD monitoring was at 215 nm for all compounds [41,42].The standard curve was obtained using the linear regression method and peak areas were plotted versus concentrations. The regression equation was $y = 28.698x - 9.4848$ ($r^2 = 0.9994$) in the concentration range of 0.005–0.3 mg mL^{-1} for the standard kirenol.

2.3. Preparation of MIPs and NIPs

The polymers were prepared through thermal polymerization with a non-covalent approach. Kirenol as the template and the AM as the functional monomer were dissolved in 25 mL THF in 50 mL round-bottomed flask, and kept at 100 rpm rotation for 5 h in room temperature. Then, cross-linker EGDMA and free-radical initiator AIBN (24 mg) were added. The mixture was degassed in an ultrasonic bath for 15 min, and filled with oxygen-free nitrogen for 10 min and sealed by means of a rubber plug. The flask was then placed in water bath and the mixture was thermally polymerized at 60 °C for 24 h. The resultant polymers were grounded and sieved through a 200 mesh stainless steel sieve (particle size less than 75 μm). The polymer particles were extracted using a soxhlet apparatus in methanol–acetic acid solution (9:1, v/v) for 24 h to remove the template and then washed by methanol for washing out the acetic acid and dried in vacuum overnight at 40 °C. The NIPs were prepared in the same method as MIPs but without the addition of template.

The surface morphologies of the MIPs/NIPs were observed via a Hitachi S-4800 field emission scanning electron microscope (Tokyo, Japan) and their FT-IR spectra were obtained via a Nicolet Nexus-670 FT-IR spectrometer. The wave numbers of FT-IR measurement range were controlled from 500 cm^{-1} to 4000 cm^{-1}.

2.4. Binding experiment and selectivity evaluation

The adsorption test was aim to evaluate the capacity of MIPs for recognizing and binding kirenol in THF.

Adsorption kinetic studies were performed as follows: 40 mg of MIPs or NIPs were weighed into kirenol solution (1.0 mL, 20 mg L^{-1}) in 2 mL centrifuge tube and sealed. The tubes were oscillated by a SHA-B incubator (100 rpm) (Jintan Zhengji Instrument Co., Ltd., Jiangsu, China) at 35 °C for different time intervals (for 0.5, 1.0, 2.0, 4.0, 8.0, and 12.0 h, respectively). The solutions were centrifuged, filtered, and then determined using HPLC.

Static adsorption experiments were carried out as following: 40 mg of MIPs or NIPs were suspended in 1 mL of various concentrations of kirenol solution (5 mg L^{-1} to 30 mg L^{-1}) in 2 mL centrifuge tube. The tubes were sealed and then shaken in SHA-B incubator for 5 h at 35 °C. The concentrations of free kirenol were determined using HPLC. The data of the static absorption experiment were further processed according to the Freundlich isotherm (FI) model (Eq. (1)) to estimate be binding parameters of the MIPs, which is reflected in linear log *B* versus log *F* plots according to Eq. (2):

$$B(F) = a F^m \tag{1}$$

$$\log B = m \log F + \log a \tag{2}$$

where *B* and *F* are the concentrations of bound and free analyte, respectively, and *m* is the so called heterogeneity index. The parameter *m* can take values from 1 to 0, increase with decreasing heterogeneity of the material. The broad applicability of the FI to non-covalent MIPs has been demonstrated recently [43]. The affinity distribution (AD) can be calculated using Eq. (2) and the experimentally derived FI fitting parameters (*a* and *m*) [44]

$$N(k) = 2.303\, am(1 - m^2)K^{-m} \tag{3}$$

where *K* is the affinity constant (*K* can be assumed to be equal to *1/F*) and $N(k)$ is the number of binding sites with a given affinity.

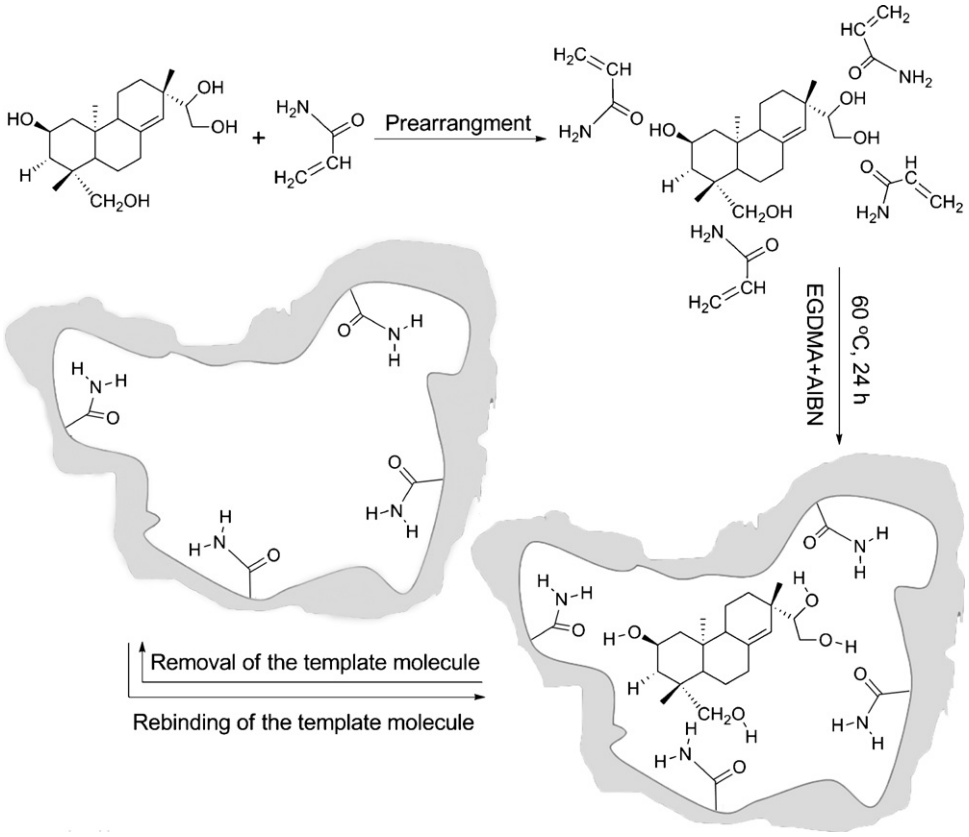

Fig. 2. Schematic representation of kirenol-MIPs.

The number of binding sites ($N_{k\min-k\max}$; see Eq. (4)) and the weighted average affinity ($K_{k\min-k\max}$; see Eq. (5)) can be calculated where a and m is equivalent to the Freundlich parameters [44]:

$$N_{k\,\min-k\,\max} = a(1-m^2)(K_{\min}^{-m} - K_{\max}^{-m}) \quad (4)$$

$$K_{k\,\min-k\,\max} = \left(\frac{m}{m-1}\right)\left(\frac{K_{\min}^{1-m} - K_{\max}^{1-m}}{K_{\min}^{-m} - K_{\max}^{-m}}\right) \quad (5)$$

The values for these parameters can be calculated from the experimental maximum free analyte concentrations ($F_{\max}$) and minimum free analyte concentrations ($F_{\min}$) and within the limits of $K_{\min}$ and $K_{\max}$ being equal to the reciprocal corresponding concentrations $K_{\min} = 1/F_{\max}$ and $K_{\max} = 1/F_{\min}$.

40 mg of MIPs or NIPs were added into 2 mL centrifuge tube, and 1 mL, 20 mg L^{-1} kirenol, darutigenol, TD or PA solution was also added to evaluate the selectivity of the imprinted sorbent. The mixtures were shaken in SHA-B incubator for 5 h at 35 °C. The concentrations of free analyte were determined using HPLC.

2.5. MIP/NIP-SPE procedures

2.5.1. Preparation of the MI/NI-SPE column

An empty column (6 mL total volume, 1 cm diameter) was employed as the MI/NI-SPE column. The column was packed with wet-filling. 100 mg of dry kirenol-MIPs were added to 5 mL methanol and the mixed solution was filled into the 6 mL SPE column. Prior to loading the sample, the cartridge was washed with a mixture of methanol and acetic acid until kirenol could not be detected by HPLC analysis. Then each cartridge was conditioned with methanol (5 mL) and acetonitrile (5 mL).

2.5.2. Evalutation of the MISPE selectivity

In order to investigate the selectivity of MISPE protocol, a mixture containing PA, kirenol, and its analogue darutigenol, TD, and KA was prepared in acetonitrile. 1.5 mL of the mixture (5 mg L^{-1} for each) was loaded onto the MI or NI-SPE cartridge. The cartridge was then washed with 5 mL acetonitrile to eliminate molecules retained by non-specific interactions with the polymer, and the elution of the analytes was performed using 5 mL methanol–acetic acid (9:1, v/v). The collected loading solution, washing solution and elution solution were evaporated to 300 μL before analysis using HPLC.

2.6. Extraction of kirenol from extract of S. pubescens herb by MISPE

1.5 mL real sample of extract of *S. pubescens* herb was evaporated to dryness and re-dissolved in 1.5 mL acetonitrile. The obtained solution was loaded on the conditioned MI or NI-SPE cartridge. Similarly, the collected loading solution, washing solution and elution solution were evaporated to 300 μL before analysis using HPLC.

3. Results and discussion

3.1. Polymerization of MIPs

The obtained MIPs were synthesized through copolymerization of AM and EGDMA in the presence of kirenol (template) using the non-covalent imprinting approach. The non-covalent interactions are usually more easily employed because of its rapid recognition kinetics and the simplicity of the process [45].

Molecular recognition of the template molecule by imprinted polymers is based on the intermolecular interaction between the template molecule and functional groups in the polymer [46]. Different monomers, such as AM and methacrylic acid, were selected

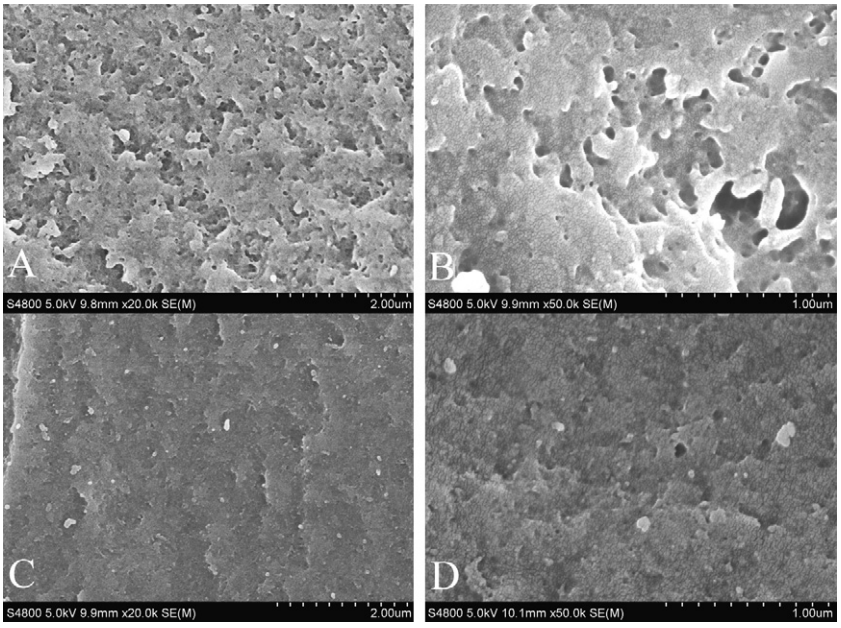

Fig. 3. Scanning electron micrographs of the MIPs and NIPs. (A) MIPs, (B) an enlarged view of image A, (C) NIPs and (D) an enlarged view of image B.

to evaluate the specific recognition ability of MIPs for kirenol molecule. The resulted polymers prepared using AM had better molecular recognition in polar conditions, and the imprinting process is shown in Fig. 2. The optimum molar ratio of 1:6:30 (template:AM:EGDMA) was used to prepare MIPs, and the stable pre-polymerization complex between the template and the functional monomer could be formed with the excess AM versus the kirenol amount in the pre-polymerisation mixture [27].

The preparation of MIPs in different polar porogenic solvents was investigated, because kirenol is a strong polar molecule that does not possess any hydrophobic functional group. The results showed that MIPs prepared in THF had higher recognition ability than that in N,N-dimethylform amide or acetonitrile: methanol (1:1, v/v). The strong cohesion between kirenol and AM led to the successful imprinting of kirenol with the decomposing action made by THF. Fig. 3 shows the surface morphologies of MIPs and NIPs via SEM. Particles of the MIPs (Fig. 3A and B) exhibited a more porous, larger pore size, and rough structure than that of NIPs (Fig. 3C and D). The MIPs with uniform and more open structure is obviously favorable for the adsorption of the large template molecules of kirenol.

To further ensure that the kirenol-MIPs had been prepared, FT-IR analysis was performed. In Fig. 4, the characteristic peak of AM was around at 3354 (and 3188), 1674, and 1612 cm^{-1}, corresponding to the N—H, C=O and C=C stretching of AM. The absorbance peak of C=O at 1730 cm^{-1} in the MIP spectrum shows that the MIPs were synthesized through the polymerization of EGDMA and AM. The weak absorbance peaks of C=O and C=C at 1677 cm^{-1} and 1626 cm^{-1} demonstrated that most AM were cross-linked and only a few remained unlinked. Moreover, the peak intensity of the stretching vibration of C=O (1679 cm^{-1}) in the NIPs were lower than that of MIPs because of the impact of hydrogen between kirenol and the AM.

3.2. Recognition mechanism of MIPs

From the general formation mechanism of MIP binding sites, functional monomers are responsible for the binding interactions in the imprinted binding sites [47]. Thus, the study of the intermolecular interaction between the functional monomer and the template molecule is important.

To investigate the recognition mechanism, different ratios of AM to kirenol was dissolved in THF and scanned using a UV spectrophotometry (Perkin Elmer, Lambda 35) from 190 nm to 400 nm, and the results are shown in Fig. 5. Fig. 5 shows that the maximum absorbance of kirenol absorption peaks increased with the increase of AM concentration. The maximum absorbance was obtained when the ratio of kirenol and AM was 1:6. However, with further increase in the concentration of AM, the maximum absorbance was reduced, indicating that more complicated compounds were being formed. These data provided strong evidence that hydrogen bond was formed between kirenol and AM, which led to the formation of an associated complex of kirenol and AM self assembly [47]. It could be inferred that the formation of hydrogen bonds occurred between hydroxyl of kirenol and amino of AM according to the molecular structures of kirenol and AM. Therefore, hydrogen bond would be the main binding force in the formation process of

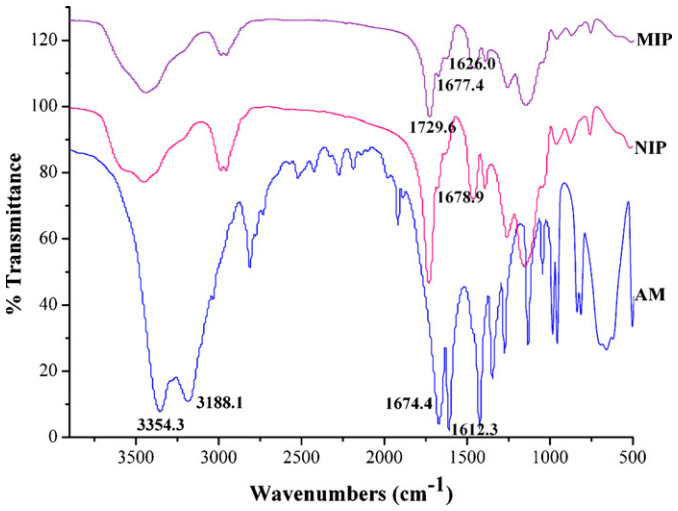

Fig. 4. FT-IR spectra of the kirenol MIP and NIP particles, AM.

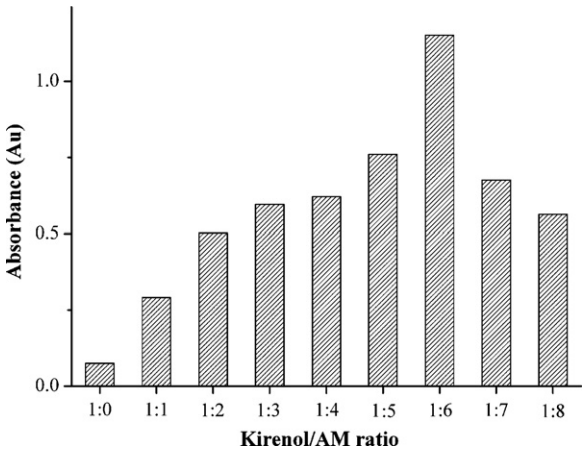

Fig. 5. The UV absorbance of different proportions of kirenol and AM.

recognition sites, and the optimum molar ratio of kirenol and AM was in agreement with the experimental result.

3.3. Adsorption kinetics and selectivity evaluation of MIPs and NIPs

Fig. 6 shows the kinetic adsorption processes of kirenol on MIPs and NIPs, where Q is the amount of kirenol adsorbed at any time. Adsorption capacity increased continuously with time and reached equilibrium within 4 h. The optimum time was set to 5 h for the adsorption equilibrium. The higher adsorption capacity of MIPs indicated that molecular imprinting had resulted in the formation and preservation of specific recognition cavities on the MIPs. For the NIPs, the non-specific adsorption played a dominant role, although there were no suitable recognition sites and imprinting cavities. Therefore, the specific adsorption of MIPs was attributed to the presence of complementary cavities to the template molecules.

The specific recognition ability was evaluated using the recognition coefficient (α). And the recognition coefficient α was defined as the ratio of the amount of analyte bound to MIPs (S_{MIP}) and NIPs (S_{NIP}) [48]. Theoretically, when α is greater than 1, MIP has selectivity to the analyte. Table 1 shows that the α of MIPs to kirenol and its analogues were greater than 1. MIPs can recognize not only the template molecules, but also structurally related compounds. The three diterpenoids have similar adsorption behaviors on MIPs. However, the α for PA was around 1, indicating that the MIPs had no specific site to the compound with significantly different structure.

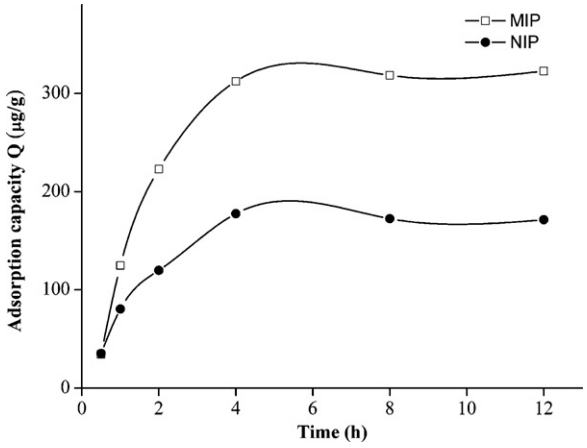

Fig. 6. Dynamic curves of the adsorption of kirenol onto MIPs and NIPs.

Table 1
Recognition coefficient of MIPs to kirenol, darutigenol,TD, and PA from static adsorption.[a]

Analytes	S_{MIP}	S_{NIP}	α
Kirenol	337.5	136.5	2.47
Darutigenol	435.0	127.0	3.43
TD	469.0	138.0	3.40
PA	78.0	78.5	0.99

[a] The concentrations of the analytes were 5 mg L^{-1}, respectively; the unit of S_{MIP} and S_{NIP} were $\mu g\,g^{-1}$; the RSDs for the data were lower than 3.1%.

Table 2
Freundlich fitting parameters, number of binding sites ($N_{kmin-kmax}$) and weighted average affinity ($K_{kmin-kmax}$) obtained with the experimental binding data of kirenol toward the MIPs and NIPs.[a]

Fitting parameters	MIPs	NIPs
$N_{kmin-kmax}$ ($\mu mol\,g^{-1}$)	1.092 ± 0.004	0.339 ± 0.001
a [($\mu mol\,g^{-1}$) ($mmol^{-1}$)^m]	1.862	1.837
$K_{kmin-kmax}$ ($L\,mmol^{-1}$)	66.07 ± 0.07	41.32 ± 0.03
K_{range} ($L\,mmol^{-1}$)	35.14 – 124.22	18.06 – 102.12
m	0.501	0.849
r^2	0.948	0.919

[a] Data are shown as means ± RSD.

3.4. Binding isotherms

Freundlich isotherm-affinity distribution analysis was employed to analyze the binding isotherms of kirenol onto the MIPs and NIPs. Table 2 summarizes the fitting parameters of the MIPs and NIPs, the number of binding sites, $N_{kmin-kmax}$, and the weighted average affinity, $K_{kmin-kmax}$, calculated using Eqs. (4) and (5). Fig. 7 shows the kirenol adsorption isotherms for the MIPs and NIPs with their corresponding experimental Freundlich isotherms and the affinity distribution of the MIPs and NIPs. The affinity distributions were plotted in terms of N (K) vs. log(K), which is a measure of the number of binding sites (N (K)) having a particular binding affinity (log(K)). The x-axis is usually potted in log(K) format to make this axis proportional to the binding energy (ΔG), and for this reason, affinity distributions are also called site-energy distributions. As can be seen, the number of sites with any given affinity energy is higher for the MIPs than that

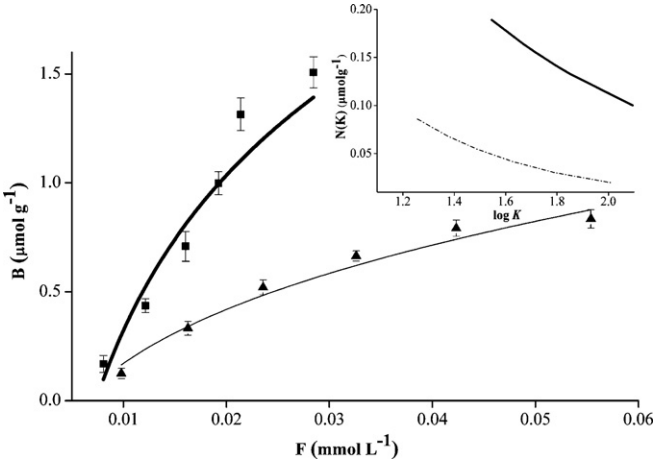

Fig. 7. Kienol adsorption isotherms for MIPs (■) and NIPs (▲) with the corresponding experimental Freundlich isotherms for MIPs (thick line) and NIPs (thin line), and affinity distributions of MIPs (–) and NIPs (- - -).

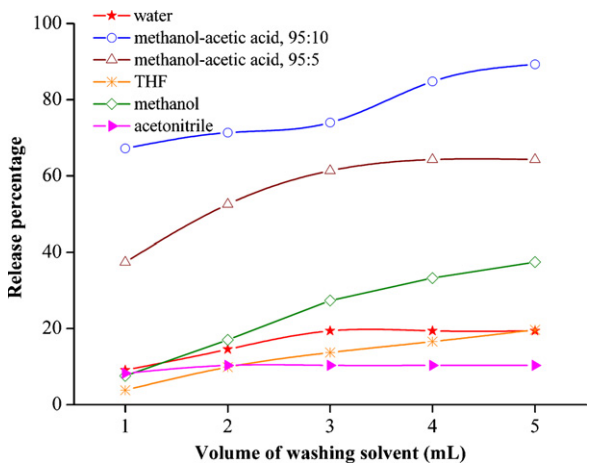

Fig. 8. Release percentage of kirenol of increasing volumes of different washing solvents through the MIP cartridge.

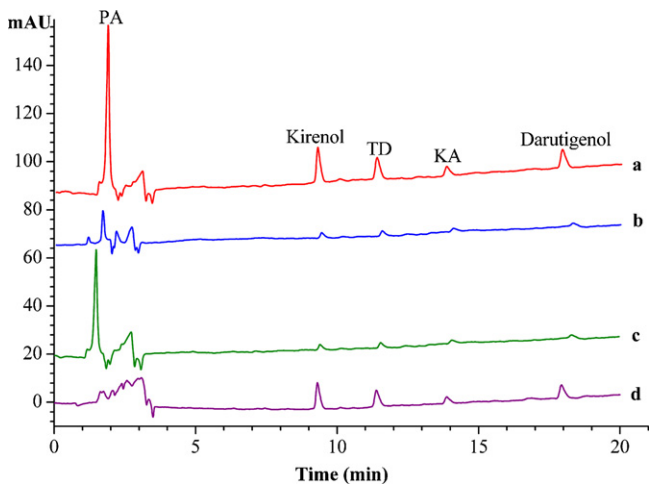

Fig. 9. Chromatograms of the standard mixtures. (a) Initial solution before MISPE, (b) solution after loading, (c) solution after washing and (d) eluate after rinsing with methanol–acetic acid (9:1, v/v).

of NIPs across the entire range of concentrations tested, thereby confirming the imprinting phenomenon.

The values of the total number of binding sites as well as the affinity constant are higher in the MIPs than in the NIPs. The value of $N_{Kmin-Kmax}$ for the MIPs is slightly higher than for the NIPs (1.092 and 0.329 μmol g^{-1}, respectively) and the value of K_{MIP} ($K_{kmin-kmax}$) = 66.07 L $mmol^{-1}$ is much higher than that of K_{NIP} ($K_{kmin-kmax}$) = 41.32 L $mmol^{-1}$. This means that the contribution of the template molecule to the total number of binding sites for each polymer is more notable. Thus it is clear that the template molecule displays an important role in the heterogeneity of the MIPs.

3.5. Evaluation of kirenol-MIPs in solid-phase extraction

The off-line MISPE protocols were used to evaluate the molecular selectivity of the MIPs and NIPs obtained in the present study as sorbents.

3.5.1. Optimization of SPE procedures

In the consideration of the loading step, the optimal solvent to be used was established. Different volumes of 5 mg L^{-1} kirenol solution (in water, THF, or acetonitrile) in the range of 0.5–2.0 mL were loaded to the MISPE column. The eluate was collected and analyzed using HPLC. The results showed that the best solvent was acetonitrile, and that the optimal volume was 1.5 mL.

In the consideration of the washing step, kirenol in acetonitrile (1.5 mL, 5 mg L^{-1}) was loaded into the cartridge as described above. The cartridge was washed with different volumes of water, acetonitrile, or THF (1.0 mL–5.0 mL). Considering the recovery of kirenol (Fig. 8) and the washing capacity of the solvent for different polar impurities in the real sample, 5 mL of acetonitrile was used as the washing solvent.

Methanol and methanol–acetic acid (95:5 and 90:10, v/v) were tested as elution solvents to release the template from MIPs. The same kirenol solution was loaded, and different volumes of the eluent between 1.0 mL and 5.0 mL were tested. The best recovery was obtained when using 5 mL methanol–acetic acid (90:10, v/v) as the elution solution (Fig. 8).

3.5.2. Selectivity of the SPE column

Based on the above optimization results, the selectivity of the MIPs was evaluated. The chromatograms of PA, kirenol, and the structurally similar darutigenol, TD, and KA obtained using the MISPE pretreated column are shown in Fig. 9. Good baseline separation was obtained without producing SPE and kirenol was eluted second (Fig. 9a). Only the apparent peak of PA was observed in Fig. 9b to determine the solutions after MISPE, which indicates that kirenol and its analogues were almost completely adsorbed onto the MIPs, although PA could not be adsorbed. Fig. 9c shows that a few kirenol and its analogues were washed from the MISPE column with acetonitrile. Fig. 8d shows that kirenol and its analogues were almost completely eluted with methanol–acetic acid (90:10, v/v). After the elution step, the elution ratio of kirenol following MISPE was almost 88% (7.4% of NIPs) (Fig. 10), while the analogues were 69.2–70.9% (7.4% to 25.2 of NIPs). The recoveries of kirenol and its analogues were low following NISPE, which is attributed to the limited retention during the washing step. These results can easily explain the spatial orientation of the functional groups in the specific binding sites as an important factor for the molecular recognition in non-covalent MIPs. MISPE exhibited highly selective binding affinity for kirenol and the capacity to rebind other structurally similar diterpenoids; however, it was lower than that for the original template.

3.6. Application of kirenol-MIPs to TCM samples

To check the applicability of the MISPE for the extraction of the selected diterpenoids in real matrices, *S. pubescens* herbs were extracted following the Chinese Pharmacopoeia and were subjected to the MIP extraction procedure. Initially, the evaluation

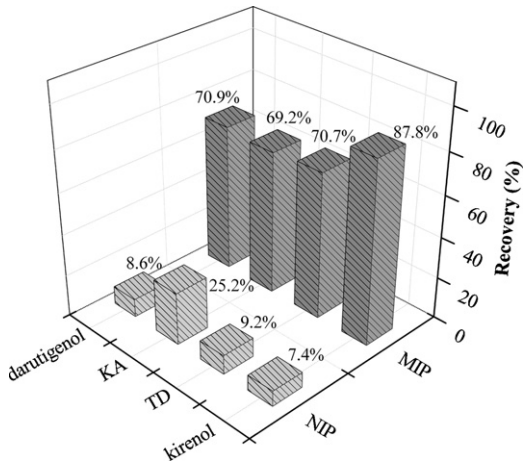

Fig. 10. Elution recoveries of four diterpenoids from MI- and NI-SPE.

Table 3
Capacity evaluation of MISPE cartridges with extracts of *S. pubescens* herb.[a]

Compound	Loaded on the cartridge (μg)	Lost during load (μg)	Lost during wash (μg)	Eluted (μg)	Recovery (%)
Kirenol	15.60	1.27	1.84	12.62	80.9 ± 2.5
TD	3.78	0.47	0.86	2.40	63.6 ± 4.7
KA	88.71	13.35	32.37	34.06	38.4 ± 5.3
Darutigenol	13.85	1.90	3.71	8.21	59.3 ± 3.4

[a] Data are shown as means ± RSD. The amounts of diterpenoids loaded on the cartridge were determined in methanol extract before MISPE.

of MIPs was performed using a 100 mg MIP cartridge. To increase the number of available binding sites of the cartridge because of the possible interferences and binding of other diterpenoids from the plant extracts on MIPs, 200 mg MIP cartridge was used. No related peak was observed in Fig. 11b in the analysis of the solutions after MISPE, which indicated that the components in the TCM extracts were almost completely adsorbed onto the MIPs. The washing solvent (acetonitrile) can eliminate effectively the polar matrix components. After the washing step, the polar matrix components were nearly discarded, and kirenol loss was 8.1% of the loading amount. An important clean up of the extracted mixture was obtained by the presence of several peaks of diterpenoids (Fig. 11d). The selective elution of diterpenoids was obtained using methanol–acetic acid (9:1, v/v), and the experimental results are reported in Table 3. The recovery of the diterpenoids after the MISPE procedure was calculated as the ratio of the amount of diterpenoids eluted using acidic solvent and the amount loaded on the MIPs. A high yield of kirenol with 80.9% satisfactory recovery was obtained from the TCM extracts by the proposed MISPE. The recoveries of the other compounds were unexpected according to the binding capacity of diterpenoids as shown in Fig. 9. The possible reason may be the strong effect of the complex sample matrix. Nevertheless, most of the polar matrices were eliminated from the MIP and NIP cartridges during the washing step.

Finally, a comparison between the MISPE and commercially available C_{18} SPE was performed. The C_{18} SPE extraction failed to selectively extract diterpenoids from the herb extracts (Fig. 12). This result revealed the suitability of the MISPE method for the selective extraction of natural diterpenoid compounds from crude TCM extracts.

Considering the accuracy of the determination of kirenol, instrument precision was evaluated through the analysis of five injections of the same elution solution. The precision of the apparatus was found to be satisfactory (RSD = 0.36%). After repetitive use of the MIP cartridge for five times, the RSD was found to be 2.8%, indicating a good reproducibility of the MIPs. According to the signal to noise ratio equal to 3.0, the limits of detection for kirenol in the herb extracts after MISPE was 0.75 μg mL^{-1}. Standard addition method was used to evaluate the recovery of the MISPE process. The test was processed by mixing 1 mL of the herb extract with 0.5 mL standard kirenol solution (30 mg L^{-1}). The recovery of the spiked solution was 91.5% ± 3.2 (n = 3). All these data demonstrated that the MISPE process is a suitable method for the enrichment and determination of kirenol in TCMs.

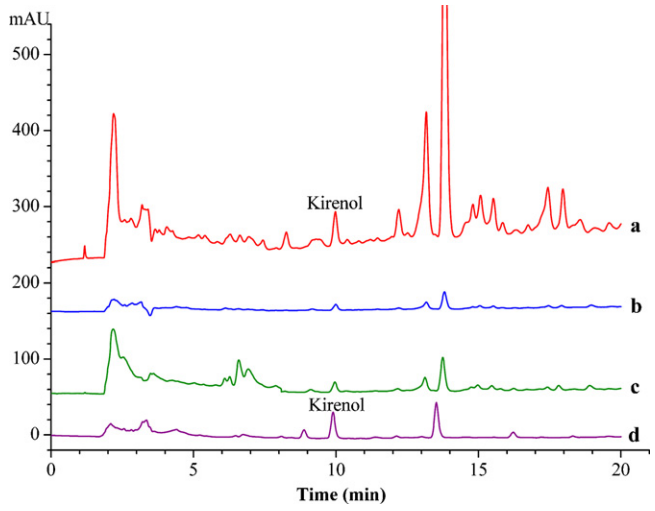

Fig. 11. Chromatograms of *S. pubescens* herb extract. (a) Initial solutions before MISPE, (b) solution after loading, (c) solution after washing and (d) eluates after rinsing with methanol–acetic acid (9:1, v/v).

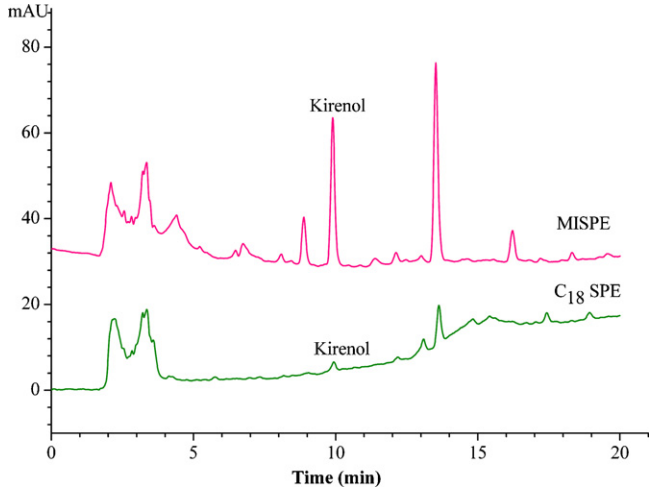

Fig. 12. Chromatograms of *S. pubescens* herbs extract after C_{18} silica SPE and after MISPE.

4. Conclusion

A molecularly imprinted polymer had been synthesized for the extraction of a diterpenoid (kirenol) from *S. pubescens* herb extracts. The MIPs were confirmed via SEM, UV–vis, and FT-IR, analyzed using HPLC–UV. The imprinting effect and selectivity of the MIPs were evaluated and the obtained polymers showed good selectivity and adsorption capacity. The MISPE was a useful tool for selective clean-up of the plant extracts, which showed excellent recovery of the template (80.9%) and is suited to routine use for diterpenoids from *S. pubescens* herb.

Acknowledgement

This work was supported by National Natural Science Foundation of China (Nos. 21075127 and 20875095).

References

[1] C.H. Lu, W.H. Zhou, B. Han, H.H. Yang, X. Chen, X.R. Wang, Anal. Chem. 79 (2007) 5457–5461.
[2] F. Priego-Capote, L. Ye, S. Shakil, S.A. Shamsi, S. Nilsson, Anal. Chem. 80 (2008) 2881–2887.
[3] H.Y. Yan, F.X. Qiao, K.H. Row, Anal. Chem. 79 (2007) 8242–8248.

[4] L. Ye, R. Weiss, K. Mosbach, Macromolecules 33 (2000) 8239–8245.
[5] J. Svenson, I.A. Nicholls, Anal. Chim. Acta 435 (2001) 19–24.
[6] C. Giovannoli, C. Baggiani, L. Anfossi, G. Giraudi, Electrophoresis 29 (2008) 3349–3365.
[7] G. Wulff, Chem. Rev. 102 (2002) 1–27.
[8] S. Azodi-Deilami, M. Abdouss, M. Javanbakht, Appl. Biochem. Biotechnol. 164 (2011) 133–147.
[9] Y.Q.Z.Y.Q. Zheng, Y.H. Liu, H.B. Guo, L.M. He, B.H. Fang, Z.L. Zeng, Anal. Chim. Acta 690 (2011) 269–274.
[10] C. Michailof, P. Manesiotis, C. Panayiotou, J. Chromatogr. A 1182 (2008) 25–33.
[11] C. Sontimuang, R. Suedee, B. Canyuk, N. Phadoongsombut, F.L. Dickert, Anal. Chim. Acta 687 (2011) 184–192.
[12] K. Haupt, A. Dzgoev, K. Mosbach, Anal. Chem. 70 (1998) 628–631.
[13] F. Lanza, B. Sellergren, Chromatographia 53 (2001) 599–611.
[14] E. Turiel, A. Martin-Esteban, Anal. Chim. Acta 668 (2010) 87–99.
[15] K. Haupt, Analyst 126 (2001) 747–756.
[16] M. Lasakova, P. Jandera, J. Sep. Sci. 32 (2009) 799–812.
[17] B. Sellergren, Anal. Chem. 66 (1994) 1578–1582.
[18] J. Yang, Y. Hu, J.B. Cai, X.L. Zhu, Q.D. Su, Anal. Bioanal. Chem. 384 (2006) 761–768.
[19] E. Caro, R.M. Marce, F.P. Borrull, a.G. Cormack, D.C. Sherrington, Trends Anal. Chem. 25 (2006) 143–154.
[20] S.A. Mohajeri, G. Karimi, M.R. Khansari, Anal. Chim. Acta 683 (2010) 143–148.
[21] J.P. Lai, R. Niessner, D. Knopp, Anal. Chim. Acta 522 (2004) 137–144.
[22] J. Jin, Z.P. Zhang, J.C. Wang, P.P. Qi, J.P. Chen, J. Sep. Sci. 33 (2010) 1836–1841.
[23] V. Pichon, F. Chapuis-Hugon, Anal. Chim. Acta 622 (2008) 48–61.
[24] T. Yang, Y.H. Li, S. Wei, Y. Li, A.P. Deng, Anal. Bioanal. Chem. 391 (2008) 2905–2914.
[25] G. Vlatakis, L.I. Andersson, R. Muller, K. Mosbach, Nature 361 (1993) 645–647.
[26] C. Baggiani, L. Anfossi, C. Giovannoli, Anal. Chim. Acta 591 (2007) 29–39.
[27] C. Lopez, B. Claude, P. Morin, J.P. Max, R. Pena, J.P. Ribet, Anal. Chim. Acta 683 (2011) 198–205.
[28] L.J. Schwarz, B. Danylec, Y.Z. Yang, S.J. Harris, R.I. Boysen, M.T.W. Hearn, J. Agric. Food Chem. 59 (2011) 3539–3543.
[29] C.Y. Chen, C.H. Wang, A.H. Chen, Talanta 84 (2011) 1038–1046.
[30] F.F. Chen, G.Y. Wang, Y.P. Shi, J. Sep. Sci. 34 (2011) 2602–2610.
[31] H.J. Park, I.T. Kim, J.H. Won, S.H. Jeong, E.Y. Park, J.H. Nam, J. Choi, K.T. Lee, Eur. J. Pharmacol. 558 (2007) 185–193.
[32] H.M. Kim, C.Y. Kim, M.H. Kwon, T.Y. Shin, E.J. Lee, Arch. Pharm. Res. 20 (1997) 122–127.
[33] J.E. Huh, Y.H. Baek, J.D. Lee, D.Y. Choi, D.S. Park, J. Pharmacol. Sci. 107 (2008) 317–328.
[34] J.P. Wang, J.I. Ruan, Y.L. Cai, Q. Luo, H.X. Xu, Y.X. Wu, J. Ethnopharmacol. 134 (2011) 1033–1038.
[35] B.H. Liu, T. Han, F.Q. Xu, J.Q. Liu, J. Anhui Tradit. Chin. Med. Colg. 26 (2007) 51–52.
[36] D.Y. Liu, H.H. Hu, China Pharm. 19 (2008) 1876–1877.
[37] H. Xin, J. Bi, M. Liu, W. Lin, R. Qian, Chin. Tradit. Herb. Drugs 36 (2005) 866–870.
[38] B.I. Juan, H.L. Xin, Z.F. Gao, W.H. Lin, Chin. Tradit. Herb. Drugs 38 (2007) 1207–1210.
[39] Sh.H. Liao, B.Y. Liao, X.M. Huang, Chin. Pharm. Aff. 25 (2011) 596–597.
[40] R. Wang, W.H. Chen, Y.P. Shi, J. Nat. Prod. 73 (2010) 17–21.
[41] X.L. Song, Q.Y. Zhang, Z.M. Wang, H.Z. Fu, R.Q. Qian, Biomed. Chromatogr. 25 (2011) 542–546.
[42] Z. Liu, G.X. Chou, Zh.T. Wang, China J. Chin. Mater. Med. 35 (2010) 729–731.
[43] R.J. Umpleby, S.C. Baxter, M. Bode, J.K. Berch, R.N. Shah, K.D. Shimizu, Anal. Chim. Acta 435 (2001) 35–42.
[44] A.M. Rampey, R.J. Umpleby, G.T. Rushton, J.C. Iseman, R.N. Shah, K.D. Shimizu, Anal. Chem. 76 (2004) 1123–1133.
[45] K. Mosbach, O. Ramstrom, Biotechnology 14 (1996) 163–170.
[46] Z. Sun, W. Schussler, M. Sengl, R. Niessner, D. Knopp, Anal. Chim. Acta 620 (2008) 73–81.
[47] H.W. Sun, F.X. Qiao, J. Chromatogr. A 1212 (2008) 1–9.
[48] K.G. Yang, Z.B. Liu, M. Mao, X.H. Zhang, C.S. Zhao, N. Nishi, Anal. Chim. Acta 546 (2005) 30–36.